Applied Surface Science 390 (2016) 7–16

Contents lists available at ScienceDirect

Applied Surface Science

journal homepage: www.elsevier.com/locate/apsusc

Interaction between bimetal cluster Ni_2Co_2 and MgO and its effect on H adsorption and H_2 dissociation: A DFT study

Kai Li[a], Hongyan Liu[a,b], Riguang Zhang[a], Lixia Ling[a,c], Baojun Wang[a,*]

[a] Key Laboratory of Coal Science and Technology of Ministry of Education and Shanxi Province, Taiyuan University of Technology, No. 79 Yingze West Street, Taiyuan 030024, Shanxi, PR China
[b] College of Chemistry and Environmental Engineering, Shanxi Datong University, No. 1 Xingyun Street, Datong, Shanxi 037009, PR China
[c] College of Chemical Engineering, Taiyuan University of Technology, No. 79 Yingze West Street, Taiyuan 030024, Shanxi, PR China

ARTICLE INFO

Article history:
Received 21 June 2016
Received in revised form 28 July 2016
Accepted 8 August 2016
Available online 10 August 2016

Keywords:
Density-functional theory
Metal-support interaction
Hirshfeld charge
Adsorption energy
H_2 dissociation

ABSTRACT

It is investigated for the interactions of bimetal NiCo with MgO as well as its effects on the H adsorption and H_2 dissociation using a density functional theory method. Two models, Ni_2Co_2 cluster supported on perfect MgO(001) and oxygen-vacancy MgO(001) are used to represent bimetal NiCo deposited on MgO catalysts. The results show that the Ni_2Co_2/MgO catalyst with oxygen-vacancy exhibits stronger metal-support interaction compared to the perfect Ni_2Co_2/MgO, however, it has the weaker H adsorption ability as well as the better H_2 dissociation activity. Compared with Ni_4/MgO, the interaction between metal and support is weaker on the corresponding Ni_2Co_2/MgO, and H adsorption is stronger as well as the H_2 dissociation is accelerated. The results indicate that both addition of a second metal Co and modification the support MgO can tune the metal-support interaction, further to change the H adsorption ability, meanwhile improve the activity of H_2 dissociation. This work finely identifies the experimental result that tune the metal-support interaction can improve the catalyst's performance.

1. Introduction

Metal-support interaction is fundamental important for heterocatalyst, because the interaction can change the performance of catalyst. In general, the interaction exists in transition metal supported on oxide support surfaces [1–5], such as MgO, Al_2O_3 and SiO_2. For example, Hu et al.[6–9] found that a Ni/MgO catalyst had excellent anti-coking performance, which was partly attributed to the strong Ni-MgO interaction.

Recently, it is considered as one of the hot issue to focus on tuning metal-support interaction, further modifying the catalytic properties [10,11]. Tsang et al. [12] fine-tuned the catalytic properties of Pd by rationally varying the metal-support interaction through the formation of bimetallic nanoparticles. The metal-support interaction also can be evaluated by density functional theory method, Wang et al.[13] calculated and obtained that the binding energies are 0.8, 1.1, 2.0 and 0.8 eV for metal (metal = Ni, Pd, Pt or Cu) on perfect MgO surface and 1.1, 2.6, 3.7 and 0.8 eV in metal and MgO with an oxygen vacancy.

H adsorption, H_2 dissociation or formation are widely involved in the reactions catalyzed by Ni-based catalysts, such as CO methanation, CO_2 methanation, CH_4/CO_2 reforming, CH_4/H_2O reforming and so on. Ni-based catalysts are effective for the above reactions. However, carbon deposition is disadvantage for the activity and life of Ni-based catalysts in above reactions. In order to avoid carbon deposition, three ways are conducted to tune metal-support interaction, further to keep the reaction continue. The three ways are as follows: *(i)* addition a second metal, such as Fe, Co and Cu, to Ni-based catalysts *(ii)* selecting different support, such as MgO, SiO_2, Al_2O_3 for the Ni-based catalysts *(iii)* addition promoter to Ni-based catalysts. For example, A. Djaidia et al. [14] added M (M = Fe or Cu) to Ni/MgO and proved that the bimetallic catalysts have high performances and a good resistance for coke formation. Zhang et al. [15] have compared four Ni-based bimetallic catalysts Ni-M-Al_2O_3-MgO (M = Mn, Fe, Co and Cu), and concluded that Ni-Co bimetallic catalyst has superior performance in respect of activity and stability compared to other Ni-M combinations. The good performance of the catalysts results from not only the synergy effect between Ni and a second metal, but also metal-support interaction. Is it advantageous for the interaction between metal and support to increase or decrease for the reaction? Hossain et al. [16] found that the activation of energy of hydrogen desorption for Co-Ni/Al_2O_3 is less than that of unpromoted Ni/Al_2O_3 samples, this is mainly because that

* Corresponding author at: No. 79 Yingze West Street, Taiyuan 030024, PR China.
E-mail address: wangbaojun@tyut.edu.cn (B. Wang).

http://dx.doi.org/10.1016/j.apsusc.2016.08.045
0169-4332/

Co might promote the performance of Co-Ni/Al_2O_3 particles by reducing the metal-support interactions. However, Cui et al. [17] claimed that moderate metal-support interaction is necessary to ensure the high activity and stability of the Ni/Al_2O_3 catalyst for syngas methanation.

The metal-support interaction effects on catalytic performance may be from two respects. One is that it affects the electron structure of metals, the other is that it changes catalyst's geometric properties. Mineva et al. [18] obtained that small electron transfer of 0.2–0.3 *e* from the support MgO to the metal Rh or Pd by DFT calculation. On the other hand, Koningsberger et al. [19] proposed that the morphology of the metal clusters change is related to the interaction between metal-support by means of X-ray absorption technique. Sterrer and his co-workers [20] observed an long-range ordered Au array on the MgO surface, which indicates that charges transfer between the substrate and Au.

For MgO supported Ni-based bimetal catalysts, there is only a little work focused on the tuning the interaction of metal-support, further tuning the catalysts' performance. The detailed contributions about the active component-support structures, the electron transfer between metal and MgO as well as the metal-support effect on the reaction, are scarce. Therefore, we need address this problem herein. One approach is to rely on so-called model catalysts. The results based on the model catalysts become possible to correlate the geometric and electronic structures as well as the related adsorption properties and reaction mechanisms at a high level of detail [21–23]. Here, we apply this model approach to the important class of nickel-cobalt bimetal cluster loaded on MgO catalysts. The non-polar (001) surface of magnesium oxide is the most studied one [24–26]. Its relatively simple structure does not undergo significant relaxation or reconstruction and can provide a good model for describing deposited transition metal atoms as well as adsorption features of small molecules. In addition, point defect involved O-vacancy on the oxide surface was discussed.

Recently, density functional theory (DFT) studies have shown that the existence of oxide supports considerably affect the chemical reactivity of the metal catalyst on Ni-based catalysts because of the metal-support interaction [27–29]. Our previous work reported that Ni_4 supported on nanosized MgO was highly stable and active in CH_4/CO_2 reforming via DFT method [30]. In the present work, theoretical methods based on quantum chemistry can provide electronic and atomic level information that cannot be easily obtained by experimental methods. Therefore, we carried out DFT calculations with periodic slab model on the interactions between Ni-based bimetals (Ni_2Co_2) and MgO surfaces as well as their effects on H adsorption and H_2 dissociation, and compared those on Ni_4/MgO. Our aims are: (1) to provide a precise evaluation of the interaction between bimetal NiCo and support MgO; and (2) to clarify the mechanism of H adsorption and H_2 dissociation on NiCo/MgO; (3) to analysis their corresponding electronic nature; (4) to figure out the metal-support interaction effects on H adsorption and H_2 dissociation.

2. Computational details

2.1. Computational model

Li et al. [31] used Ni_4/γ-Al_2O_3(100) model to represent Ni supported on Al_2O_3 surface. Based on the above model, they investigated the dissociation of CH_4 and H_2. In our previous work [30], two models, Ni_4 cluster supported on perfect MgO(001) and oxygen-vacancy MgO(001) were used to represent catalysts of Ni deposited on MgO. The crystallographics axis of MgO surface as well as Ni_4/MgO structures and the corresponding parameters are shown in Fig. 1. Fig. 1(a) represents the crystallographics axis of MgO surface, Fig. 1(b) represents the perfect Ni_4/MgO model, and Fig. 1(c) represents the defective Ni_4/MgO model. In the models, four different sites where deposited metals are marked as *a*–*d*, respectively.

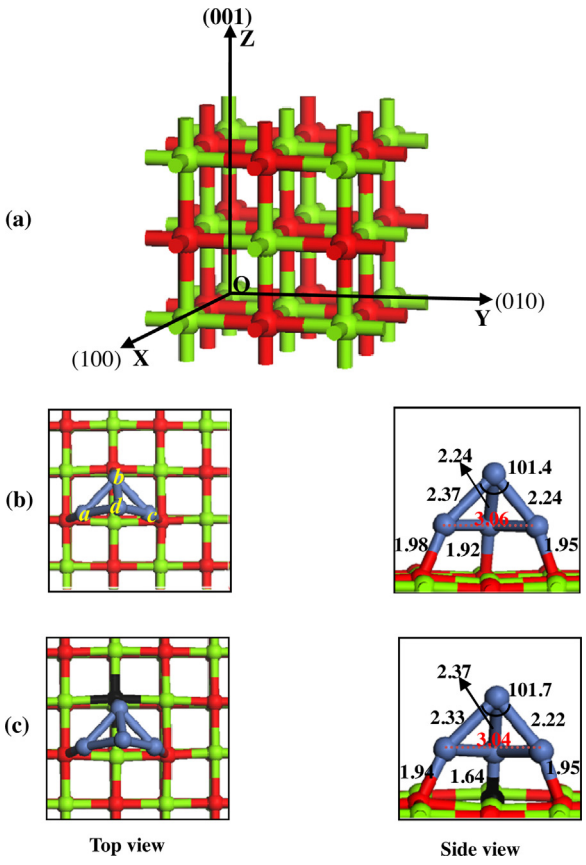

Fig. 1. The crystallographics axis of MgO surface as well as top and side views of Ni_4 supported on perfect and defective MgO(001) surface. (a) the crystallographics axis of MgO surface (b) perfect Ni_4/MgO (c) defective Ni_4/MgO. (The blue spheres: Ni; the green spheres: Mg; the red spheres: O; the black spheres: O-vacancy) (Bond lengths are in Å and dihedral angles are in °). (For interpretation of the references to color in this figure legend, the reader is referred to the web version of this article.)

Because it was reported that NiCo bimetal active component with Co/Ni ratio to unit showed the good performance in carbon dioxide reforming of methane [15,32]. We selected two Co atoms substitute for two Ni atoms in Ni_4/MgO(001) as the model of NiCo bimetal supported on perfect MgO. Therefore, four possible models for Ni_2Co_2/MgO(001) were obtained, designated as Model 1–4, and depicted in Fig. 2.

The defective Ni_2Co_2/MgO model catalysts are established by removing a neutral oxygen atom from the surface of MgO under the sites of *a*–*c* based on the most stable model of perfect Ni_2Co_2/MgO, respectively. They are denoted as De-Model 1–1, De-Model 1–2 and De-Model 1–3 in turn, and shown in Fig. 3.

Other model parameters for Ni_2Co_2/MgO are as follows, the same as those for Ni_4/MgO(001) [30]. The calculations being periodic in three dimensions, a vacuum of 12 Å was imposed between two consecutive slabs in order to eliminate any noticeable interaction with the periodic image along the *z* direction. The bottom two layers were frozen in their bulk positions, whereas the remaining two layers together with Ni_2Co_2 and the adspecies were allowed to relax in all calculations.

2.2. Computational methods

All the calculations were performed in the framework of the density functional theory (DFT) by using the Cambridge Sequen-

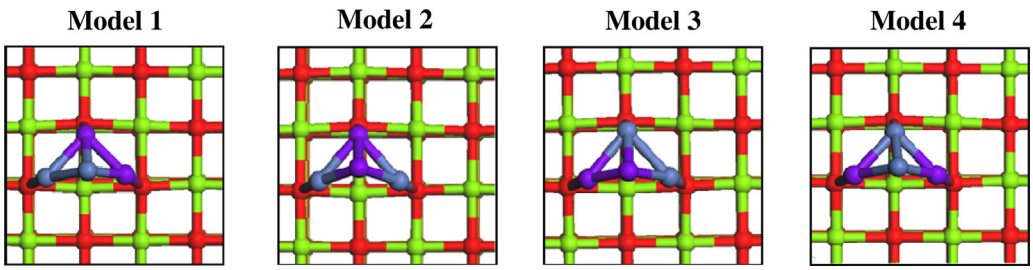

Fig. 2. Top views of Ni_2Co_2 supported on the perfect MgO(001) surface. (The purple spheres: Co; the blue spheres: Ni; the green spheres: Mg; the red spheres: O). (For interpretation of the references to color in this figure legend, the reader is referred to the web version of this article.)

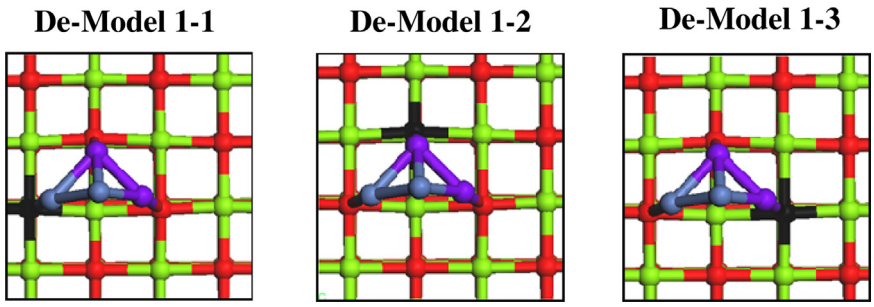

Fig. 3. Top views of Ni_2Co_2 supported on the defective MgO(001) surface. (The purple spheres: Co; the blue spheres: Ni; the green spheres: Mg; the red spheres: O; the black spheres: O-vacancy). (For interpretation of the references to color in this figure legend, the reader is referred to the web version of this article.)

tial Total Energy Package (CASTEP) [33,34] in Material Studio 5.5 of Accelry Inc. The selected calculation parameters were the same as those in our previous contribution [30,35] which is as follows: the generalized gradient approximation (GGA) has been chosen to represent the exchange-correlation potential in the formulation of the Perdew-Burke-Ernzerhof (PBE) [36]. In this framework, a large convergence of the plane wave expansion was obtained with an energy cut off of 340 eV. For geometry optimization, the Brillouin zone is sampled in a $2 \times 2 \times 1$ Monkhorst-Pack set [37]. The geometries were not optimized, until the energy, the force and the max displacement converge to 2.0×10^{-5} eV/atom, 0.05 eV/Å and 2×10^{-3} Å, respectively. Spin polarization was considered throughout all calculations.

Before adspecies adsorption, the binding energy of Ni_2Co_2 and MgO is evaluated according to the following formula:

$$E_{bin} = E(Ni_2Co_2/MgO) - E(Ni_2Co_2) - E(MgO)$$

Where $E(Ni_2Co_2/MgO)$ is the total energy of the whole system when Ni_2Co_2 is deposited on MgO, $E(Ni_2Co_2)$ and $E(MgO)$ are the energies of the isolated metal and support, respectively. The binding energy between Ni_2Co_2 and MgO can be divided into the deformation energies of Ni_2Co_2 [denoted as $E_{def}(Ni_2Co_2)$] and MgO [denoted as $E_{def}(MgO)$], as well as the interaction energy between Ni_2Co_2 and MgO (E_{inter}). Correspondingly, E_{bin} can be expressed as:

$$E_{bin} = E_{def}(Ni_2Co_2) + E_{def}(MgO) + E_{inter}$$

$$E_{def}(Ni_2Co_2) = E(Ni_2Co_2)' - E(Ni_2Co_2)$$

$$E_{def}(MgO) = E(MgO)' - E(MgO)$$

$$E_{inter} = E(Ni_2Co_2/MgO) - E(Ni_2Co_2)' - E(MgO)'$$

Where $E(Ni_2Co_2)'$ and $E(MgO)'$ are the energies of the deformed configurations of Ni_2Co_2 and MgO, respectively, when Ni_2Co_2 and MgO interacts.

The adsorption energy (E_{ads}) of adspecies is calculated as follows:

$$E_{ads} = E(ads/Ni_2Co_2/MgO) - E(Ni_2Co_2/MgO) - E(ads)$$

Where $E(ads/Ni_2Co_2/MgO)$ represents the total energy of adspecies adsorbed on Ni_2Co_2/MgO, and $E(ads)$ represents the energy of the isolated adspecies. $E(Ni_2Co_2)$ and $E(ads)$ are computed by placing them in a 10Å × 10Å × 10 Å cubic box, respectively. The adsorption energy of adspecies on Ni_2Co_2/MgO can be divided into the deformation energies of adspecies [$E_{def}(ads)$] and catalyst [$E_{def}(Ni_2Co_2/MgO)$], as well as the interaction energy between adspecies and catalyst (E_{int}). Correspondingly, E_{ads} of adspecies can be expressed as:

$$E_{ads} = E_{def}(ads) + E_{def}(Ni_2Co_2/MgO) + E_{int}$$

$$E_{def}(ads) = E(ads)' - E(ads)$$

$$E_{def}(Ni_2Co_2/MgO) = E(Ni_2Co_2/MgO)' - E(Ni_2Co_2/MgO)$$

$$E_{int} = E(ads - Ni_2Co_2/MgO) - E(ads)' - E(Ni_2Co_2/MgO)'$$

Where $E(ads)'$ and $E(Ni_2Co_2/MgO)'$ are the energies of the deformed configurations for the adspecies atom and substrate after adsorption, respectively. Meanwhile, the energy of metal-support interaction (MSI) is defined as:

$$E_{MSI} = E(ads/Ni_2Co_2/MgO) - E(ads - Ni_2Co_2)' - E(MgO)'$$

Where $E(ads - Ni_2Co_2)'$ and $E(MgO)'$ represent the energy of the unit of Ni_2Co_2 cluster and MgO substrate upon adsorption, respectively. Specially, when no adsorbed species,

$E_{MSI} = E(Ni_2Co_2/MgO) - E(Ni_2Co_2)' - E(MgO)' = E_{inter}$

In addition, the activation energy (E_a) is calculated according to the following fumula:

$$E_a = E_{TS} - E_R$$

where E_{TS} and E_R are the energies of the transition state and the reactant, respectively.

Table 1
The energy (*E*nergy, eV) of four different models of the perfect Ni_2Co_2/MgO.

	Model 1	Model 2	Model 3	Model 4
Energy	−50020.24	−50020.14	−50019.97	−50019.97

Table 2
The energy (*E*nergy, eV) of three different models of the defective Ni_2Co_2/MgO.

	De-Model 1–1	De-Model 1–2	De-Model 1–3
*E*nergy	−49580.66	−49581.24	−49580.67

The *d*-band center is calculated by the following formula [38,39].

$$\varepsilon_d = \frac{\int_{-\infty}^{\infty} E\rho(E)d\varepsilon}{\int_{-\infty}^{\infty} \rho_d(E)d\varepsilon}$$

Where ρ_d represents the density of states projected onto the Ni(Co) atoms' *d*-band; *E* is the energy of *d*-band.

3. Results and discussion

3.1. Ni_2Co_2 supported on MgO(001)

Perfect Ni_2Co_2/MgO(001) The structures of the four models of Ni_2Co_2 supported on perfect MgO are optimized, and their energies are obtained (shown in Table 1) as well as the parameters of their structures were shown in Fig. 4.

The energies reported in Table 1 are similar, i.e., the systems have similar stability; then, we have selected Model 1 as the model catalyst representing the perfect Ni_2Co_2/MgO in the following investigation, and denoted as P(Ni_2Co_2). As shown in Fig. 4, in P(Ni_2Co_2), two Co atoms (Co_b and Co_c) and one Ni atom (Ni_a) directly interact with one oxygen atoms in the MgO surface separately, while the fourth atom (Ni_d) is located at the top site away from the support surface. The Ni-O and Co-O distances are longer in Ni_2Co_2/MgO than the corresponding metal-O distances in Ni_4/MgO model. Certainly, when Co substituted Ni in perfect Ni_4/MgO, the average distance from metal cluster to MgO is stretched. It is noted that the distance of Ni_a-Co_c in Ni_2Co_2 cluster is the same long as that in Ni_4. However, the dihedral angle Ni_a-Co_b-Ni_d-Co_c is a little bigger than that in Ni_4. In addition, the distance of metal-oxygen in Ni_2Co_2/MgO and Ni_4/MgO are shorter than the distance of Ir cluster supported on MgO surface (2.6 Å) [40].

Defective Ni_2Co_2/MgO(001) The three aforementioned models of Ni_2Co_2 on the defective MgO surface were optimized. The corresponding geometrical energies are listed in Table 2. The models present similar energy, the minimum corresponds to De-Model 1–2, which is denoted as D(Ni_2Co_2). Because O-vacancy exists in MgO surface, there are only two metal-oxygen bonds between Ni_2Co_2 and MgO. The distances of the metal-oxygen in D(Ni_2Co_2) are shorter than the corresponding distances of the metal-oxygen in P(Ni_2Co_2). Meanwhile, the distance of Co_b-vacancy is 1.56 Å. In our previous contribution, the interaction of NiM (M = Mn, Fe, Co and Cu) bimetals with MgO(100) were investigated [41]. In that work, the bimetals only includes two atoms, *i.e.*, one Ni atom and one M atom. When oxygen vacancy exists in MgO(001) surface, the distance of metal to oxygen-vacancy in MgO is shortened to 1.50 Å compared that (1.95 Å) from metal to oxygen in perfect MgO, consistent with our present calculation. In addition, the distance between site *a* and *c* is slightly shorter than that in D(Ni_4).

3.1.1. Interactions between Ni_2Co_2 and MgO(001) surface

The extent of interaction between Ni_2Co_2 and MgO(001) is coarsely represented using the binding energy. The binding energies are given in Table 3. Certainly, D(Ni_2Co_2) model is more stable than P(Ni_2Co_2). Similar finding is presented between D(Ni_4) and P(Ni_4). The result also is confirmed by experimental and theoretical investigations [42,43]. On the other hand, the binding energies are weaker when two Ni atoms in active component substituted by two Co atoms, indicating that Co addition can reduce the interaction between the Ni and the support MgO. Our result is in agreement with Kang et al. [44] They have investigated Ni_4 and Ni_3Fe deposited on γ-Al_2O_3(110) surface and the result showed that the binding energies of the supported Ni_4 and Ni_3Fe are −4.98 eV and −4.80 eV, respectively, suggesting that Fe addition can reduce the interaction between the Ni cluster and the support.

Table 3
The binding energies (E_{bind}, eV), the energy of strong metal-support interaction (E_{inter}, eV) and the deformation energies (E_{def}, eV) of Ni_2Co_2 and Ni_4 on MgO(001); Hirshfeld charge(*e*) of Ni_2Co_2 and Ni_4 transferred from MgO(001).

	P(Ni_2Co_2)	D(Ni_2Co_2)	P(Ni_4)	D(Ni_4)
E_{bin}	−3.07	−4.43	−3.21	−4.70
E_{def}(MgO)	0.64	0.67	0.68	0.63
E_{def}(Ni_2Co_2 or Ni_4)	−0.14	−0.05	−0.11	−0.03
E_{inter}	−3.57	−5.05	−3.78	−5.30
Hirshfeld charge for metal cluster	−0.21	−0.35	−0.23	−0.37

In order to elucidate the interaction between Ni_2Co_2 and MgO exactly, the binding energy is divided into three parts. They are the deformation energies of isolated Ni_2Co_2 and MgO as well as the interaction energy between Ni_2Co_2 and MgO, shown in Table 3. It is clear that the deformation of MgO has the minus effect on the binding energy of metal and support, which is consistent with the literature [45–48]. However, the deformation of Ni_2Co_2 has the positive effect on the binding energy. Further, Ni_2Co_2 deformation energies have slight effect on the binding energy. Importantly, the metal-support interaction has the main effect on the binding energy. From Table 3, one can conclude that whether in Ni_2Co_2/MgO or in Ni_4/MgO, the metal-support interaction in oxygen-vacancy models is stronger than that in corresponding perfect models. On the other hand, after addition of Co to Ni-based catalyst, the metal-support interaction is decreased compared to the corresponding pure perfect or defective Ni_4/MgO models. Interestingly, the change tendency of interaction energy and binding energies are consistent in Ni_4/MgO and Ni_2Co_2/MgO.

3.1.2. Hirshfeld charge about P(Ni_2Co_2) and D(Ni_2Co_2)

It is understood that ultimately all catalytic effects must be electronic in the sense that chemical bonds are being formed and broken by the catalyst, and these bonds are electronic by nature [49]. In other words, the above observed relationships greatly depend on the degree of electrons transfer between Ni_2Co_2 and MgO. Therefore, in order to profound insight into the trends of the interactions between bimetals Ni_2Co_2 and MgO support, Hirshfeld charges analysis was conducted on the P(Ni_2Co_2) and D(Ni_2Co_2). The Hirshfeld charges of the deposited Ni_2Co_2 cluster on the MgO(001) surface are shown in Table 3. In order to comparison, we also list the Hirshfeld charges of the Ni_4 transferred from MgO.

According to the results listed in Table 3, one can easily find that the Hirshfeld charge of Ni_2Co_2 deposited on the perfect and defective surfaces are both negative, indicating the electrons transfer from MgO surface to Ni_2Co_2 when chemical interaction exists between Ni_2Co_2 and MgO. Furthermore, the data show a significant charges transferred to Ni_2Co_2 (−0.35 *e*) from the defective surface, which is more than that (−0.21 *e*) from the perfect surface, indicating the stronger interaction between Ni_2Co_2 and MgO is, the more transferred charges from MgO to Ni_2Co_2. Similar results can be observed from the Ni_4/MgO in our previous work [30]. In addition, the quantity of transferred charge is decreased when Co is added

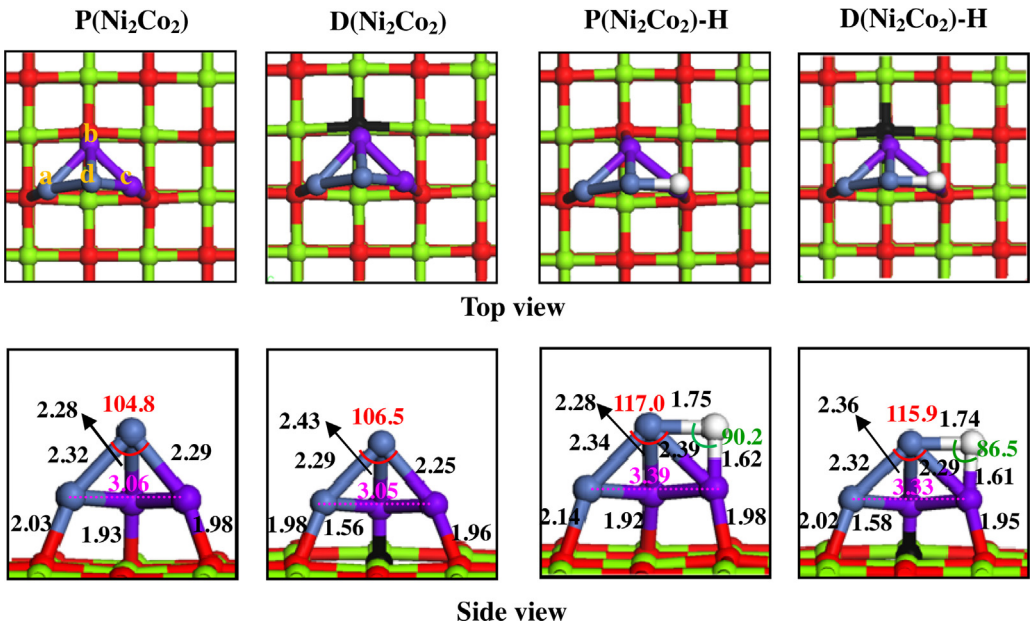

Fig. 4. The most stable configurations of the Ni_2Co_2/MgO and of H adsorbed on the substrate. (Bond lengths in Å, and dihedral angles in °; the white sphere: H atoms).

Table 4
The adsorption energies, deformation energy and interaction energy (Energy, eV) and the Hirshfeld charges (Charge, *e*) for Ni_2Co_2, Ni_4 cluster and H adsorbed on Ni_2Co_2/MgO and Ni_4/MgO.

		P(Ni_2Co_2)	D(Ni_2Co_2)	P(Ni_4)	D(Ni_4)
Energy	E_{ads}	−3.09	−2.90	−2.95	−2.84
	E_{def}(H)	0	0	0	0
	E_{def}(Ni_2Co_2/MgO Ni_4/MgO)	0.12	0.11	0.07	0.06
	E_{int}	−3.21	−3.01	−3.02	−2.90
	E_{MSI}	−3.79	−5.14	−3.54	−5.09
Charge	H	−0.11	−0.10	−0.10	−0.06
	Ni_2Co_2 or Ni_4	−0.13	−0.25	−0.13	−0.31

to active component Ni, accordingly, the interaction is weaker, *i.e.*, the binding energy is lower.

3.1.3. PDOS analysis about P(Ni_2Co_2) and D(Ni_2Co_2)

We also analyzed the *d*-band structure of Ni_2Co_2 supported on MgO, and compared with the Ni_4 supported on MgO.

The calculated *d*-band centers of Ni_2Co_2 and Ni_4 are shown in Fig. 5. Certainly, the *d*-band centers of P(Ni_2Co_2) and D(Ni_2Co_2) farther downshift from the Fermi level compared to the corresponding *d*-band centers of P(Ni_4) and D(Ni_4) [30]. In general, the closer the *d*-band center to the Fermi level, the more reactive is the catalyst [38]. Therefore, the possible activity order of the four model catalysts is: D(Ni_4) > P(Ni_4) > D(Ni_2Co_2) > P(Ni_2Co_2).

3.2. H adsorption

3.2.1. Geometries of H adsorbed on Ni_2Co_2/MgO

Different H adsorption configurations on Ni_2Co_2/MgO(001) substrates are explored and the most stable adsorption configurations are found and shown in Fig. 4. They are named as P(Ni_2Co_2)-H and D(Ni_2Co_2)-H for single H atom adsorbed on perfect Ni_2Co_2/MgO(001) and defective Ni_2Co_2/MgO(001), respectively. The adsorption energies (E_{ads}) are summarized in Table 4. Clearly, the bridge sites of Co_c-Ni_d are the most stable adsorption sites for H atoms over Ni_2Co_2/MgO(001). The adsorption energy of H in D(Ni_2Co_2)-H is slightly weaker than that in P(Ni_2Co_2)-H. On the other hand, our previous work on P(Ni_4) and D(Ni_4) indicated that the bond length of H-Ni is in the range of 1.57 ~ 1.74 Å, and the adsorption energies of H are −2.95 and −2.84 eV, respectively [30]. Certainly, the adsorption energies of H are increased when Co is added to Ni-based catalysts.

3.2.2. MSI effect on adsorption of H

The adsorption energy of H on P(Ni_2Co_2) is stronger than that on D(Ni_2Co_2). Interestingly, how does the metal-support interaction affect the adsorption energy of H? In order to clarify the effect of interaction between metal (Ni_2Co_2) and support MgO on H adsorption, the adsorption energy was decomposed of three parts, *i.e.*, the deformation energies of Ni_2Co_2/MgO and H as well as the interaction between H and Ni_2Co_2/MgO, shown in Table 4. For comparison, we also list the corresponding values of energies from Ni_4/MgO.

From Table 4, because the deformation of H is zero, and the deformation of substrate has a little minus effect on the adsorption energy of H, the adsorption energy of H is mainly from the interaction between H and substrate. Analyzing the connection among E_{MSI}, E_{int} and E_{ads}, we can find that the increase of metal-support interaction (E_{MSI}) in Ni_2Co_2/MgO leads to the decrease of the interaction (E_{int}) between H and substrate, further to the decrease of the adsorption energy (E_{ads}) of H for P(Ni_2Co_2)-H and D(Ni_2Co_2)-H. For P(Ni_4) and D(Ni_4), the same conclusion can be concluded. Our result is in consistent with Herrmann et al. [50] who found that the initial heat of adsorption of hydrogen on Pt/TiO_2 has a small but significant decrease because of the development of strong metal-support interaction. However, compared the corresponding values in Ni_4/MgO and Ni_2Co_2/MgO, one can obtain that, when added Co to Ni active component, the interaction between metal and support (E_{inter}) in Table 3 is decreased, further the adsorption energy of H is increased. In turn, the metal-support interaction (E_{MSI} in Table 4) becomes stronger for Ni_2Co_2/MgO. However, compared those after and before H adsorption, the interactions between Ni_2Co_2 and MgO is become stronger while it is weaker between Ni_4 and MgO, which indicates that the synergistic effect also is an important influence to the H adsorption. In addition, our result is consistent to that of Kang et al. [44]. When added Fe to Ni_4/Al_2O_3, the interaction between Ni and Al_2O_3 decreased accompanied the adsorption energy of H (−2.83 eV on Ni_4/Al_2O_3 and −2.96 eV on Ni_3Fe/Al_2O_3) increase.

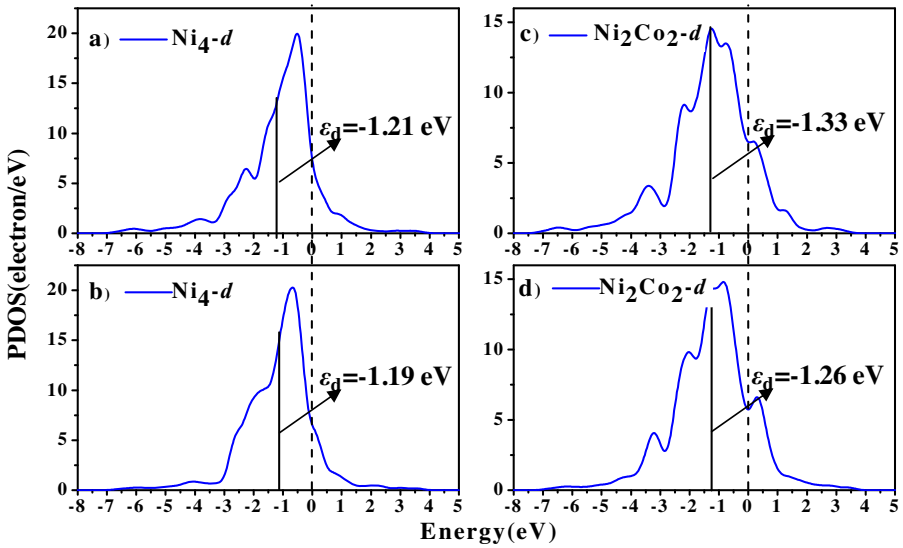

Fig. 5. The PDOS for Ni_4 and Ni_2Co_2 on MgO: (a) Ni_4 on perfect MgO; (b) Ni_4 on defective MgO; (c) Ni_2Co_2 on perfect MgO; (d) Ni_2Co_2 on defective MgO. (The location of the solid line represent the location of the *d*-band centre, the location of the dotted line represent the location of the Fermi level).

3.2.3. Hirshfeld charge about P(Ni_2Co_2)-H and D(Ni_2Co_2)-H

For further explain the effect of the metal-support interaction on H adsorption, Hirshfeld charge is analyzed, listed in Table 4. It can be seen from Table 4 that Hirshfeld charges of H are −0.11 and −0.10 *e* on P(Ni_2Co_2) and D(Ni_2Co_2), meanwhile the charges of Ni_2Co_2 are −0.13 and −0.25 *e*, respectively. Certainly, the sum of the Hirshfeld charge of H and Ni_2Co_2 after H adsorption almost equals to that of Ni_2Co_2 cluster on MgO before H adsorption. Therefore, from the electronic effect of the interaction between Ni_2Co_2 and MgO, it can be deduced that Ni_2Co_2 cluster firstly obtains electrons from the MgO support, and then transfers electrons to adspecies. Correspondingly, Ni_2Co_2 cluster on MgO acts as an electronic reservoir and conduit between the adspecies and support. The similar result is obtained by the Ni_4 supported on the MgO [30]. Due to the stronger interaction between the metal and the support results in the less charges transferred from the metal cluster to the H atom, the adsorption ability of the substrate to H is weaker, compared P(Ni_2Co_2)-H and D(Ni_2Co_2)-H. Similar results are obtained from the P(Ni_4)-H and D(Ni_4)-H.

3.2.4. PDOS analysis about P(Ni_2Co_2)-H and D(Ni_2Co_2)-H

Further, project density of state (PDOS) analysis for NiCo and H are conducted. PDOS of the *s*, *p* and *d* states of NiCo and *s* of H state for H adsorption on Ni_2Co_2/MgO are shown in Fig. 6. This figure shows that there is an orbital mixing of *s*-orbital of H atom with the *s*-, *p*- and *d*-orbital of the NiCo atoms, which is primarily in the range of −7 to 0 eV below the Fermi level. For the H adsorption on the perfect Ni_2Co_2/MgO, the area of the overlap of *s*-orbital of H and *s*-, *p*- and *d*-orbital of NiCo is bigger than the H adsorption on the defective Ni_2Co_2/MgO. The result indicates that the bonding ability between H and Ni_2Co_2 cluster on perfect MgO is stronger than that on defective MgO, which is consistent with the results of Hirshfeld charge and adsorption energy.

In addition, the order of adsorption energy of H on the catalyst is D(Ni_4) < P(Ni_4) < D(Ni_2Co_2) < P(Ni_2Co_2), contrary with that of the above calculated *d*-band center, which indicates that the adsorption becomes stronger with *d*-band center of the catalyst downshift away from Fermi level. Contrarily, in our previous investigation, on the unsupported Ni(111), the H adsorption is weaker along with *d*-band center upshift when Co is doped to pure Ni catalyst. Certainly, the MgO support affects the electronic state of active component, further affects the electronic state of adspecies, i.e., affects the ability of H adsorption, through active component transfer electrons to adspecies.

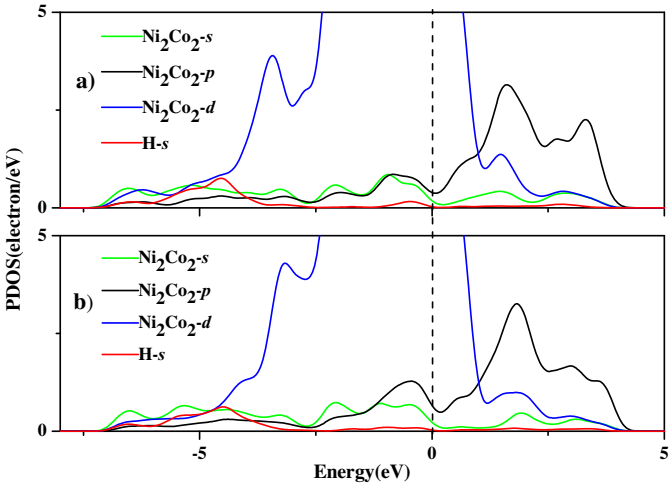

Fig. 6. The PDOS for H atom and NiCo atoms (linking to the H atom) that on MgO: (a) H atom adsorbs on the perfect Ni_2Co_2/MgO; (b) H atom adsorbs on the defective Ni_2Co_2/MgO. (The location of the dotted line represent the location of the Fermi level).

3.3. H_2 dissociation

3.3.1. H_2 adsorption

There are many possible sites for H_2 adsorption on Ni_2Co_2/MgO. Here, we only investigated H_2 adsorption on the top site of Ni_d. The most stable adsorption configuration is obtained by optimization, and shown in Fig. 7. In order to distinguish the two H atoms in H_2, we marked them as H_a, H_b, respectively. H_2 only molecularly adsorbs at the top site of Ni_d atom with adsorption energy equal to 0.05 eV and 0.01 eV on P(Ni_2Co_2) and D(Ni_2Co_2). Optimization of the isolated H_2 molecule resulted in a value of 0.75 Å for the H—H bond length. The equilibrium geometry of the adsorbed H_2 molecule shows that the H—H bond length is 0.76 Å. The adsorption energies and the bond lengths indicate the very weak interaction between H_2 and Ni_2Co_2/MgO. Similarly, the most stable structures of H_2 adsorption on Ni_4/MgO are also shown in Fig. 7. The adsorp-

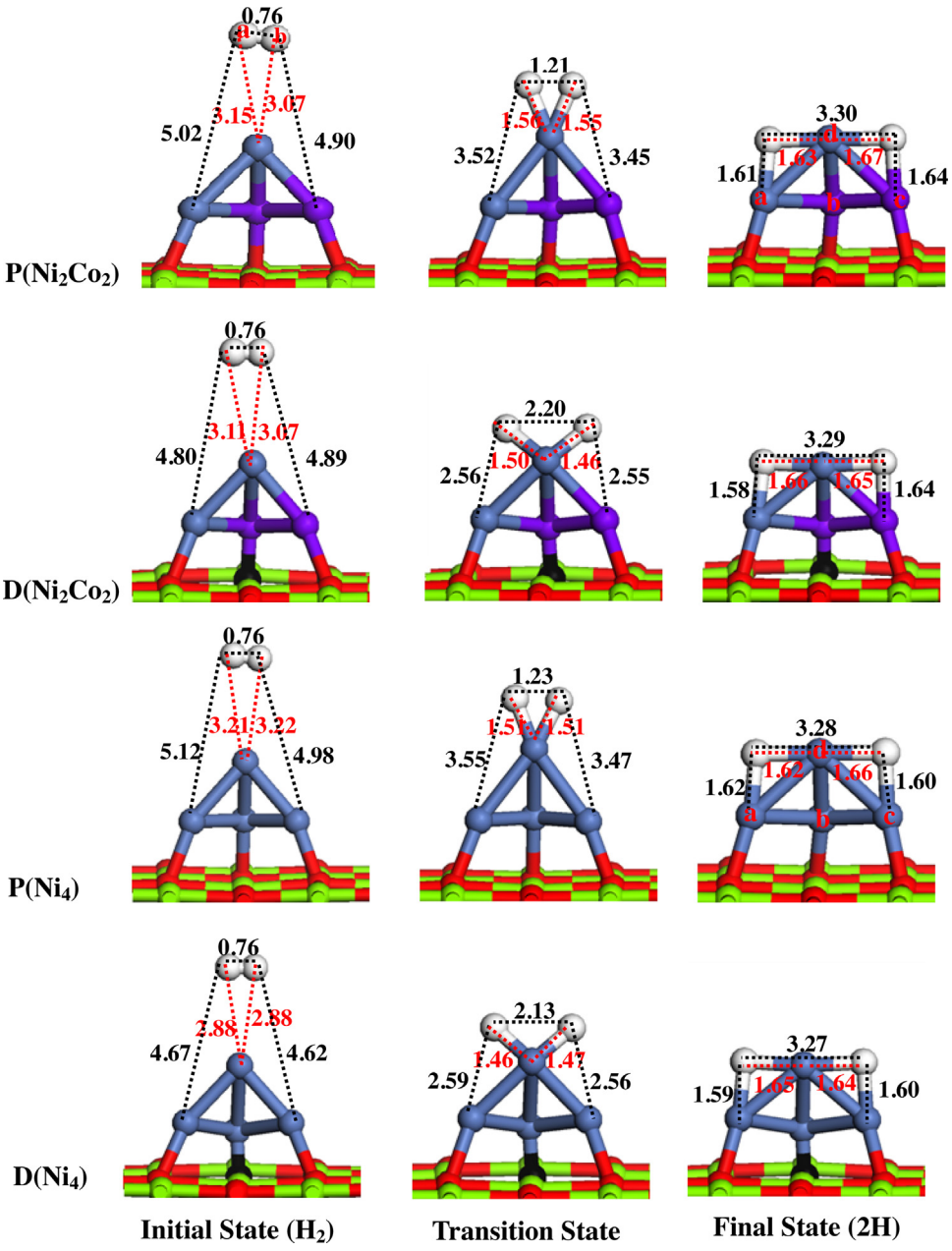

Fig. 7. Side view of the geometries structures of the initial state, transition state, and final state for H_2 dissociation and the geometrical parameters on the Ni_2Co_2/MgO(001) surfaces. (Bond lengths in Å).

tion energy of H_2 molecular adsorbed on the P(Ni_4) and D(Ni_4) are −0.08 and 0.04 eV, respectively, which is physically adsorbed. The weak interactions of H_2 on Ni_2Co_2/MgO and Ni_4/MgO do not show a significant effect from the properties of the catalysts.

3.3.2. *H + H coadsorption*

In the elementary reaction of H_2 dissociation, the final state should be the coadsorption of H and H. Therefore, we investigated the coadsorption of H and H based on the single H adsorption. The sites for the most stable coadsorption geometries of 2H upon H_2 dissociation on Ni_2Co_2/MgO and Ni_4/MgO are considered and the corresponding geometries are shown in Fig. 7 and the corresponding coadsorption energies are listed in Table 5. One H atom is adsorbed on the bridge Ni_a—Ni_d, the H—Ni_a and H—Ni_d bond are formed; the other H atom is adsorbed on the bridge Ni_c—Ni_d, the H—Ni_c and H—Ni_d bond are formed. The coadsorption geometries

Table 5
The adsorption energies, deformation energy and interaction energy (Energy, eV) and the Hirshfeld charges (Charge, *e*) for Ni_2Co_2, Ni_4 cluster and 2H coadsorbed on Ni_2Co_2/MgO and Ni_4/MgO.

		P(Ni_2Co_2)	D(Ni_2Co_2)	P(Ni_4)	D(Ni_4)
Energy	E_{ads}	−6.18	−6.23	−6.29	−6.35
	E_{def}(2H)	0	0	0	0
	E_{def}(Ni_2Co_2/MgO Ni_4/MgO)	0.31	0.20	0.19	0.15
	E_{int}	−6.49	−6.43	−6.48	−6.50
	E_{MSI}	−4.40	−5.60	−4.49	−5.90
Charge	2H	−0.19	−0.19	−0.18	−0.19
	Ni_2Co_2 or Ni_4	−0.08	−0.21	−0.06	−0.23

of 2H adsorbed on Ni_2Co_2/MgO and Ni_4/MgO are similar. The coadsorption energies of the 2H on the P(Ni_4) and D(Ni_4) are higher than those on Ni_2Co_2/MgO, meanwhile, the coadsorption energies of the two H atoms adsorbed on the defective surface are

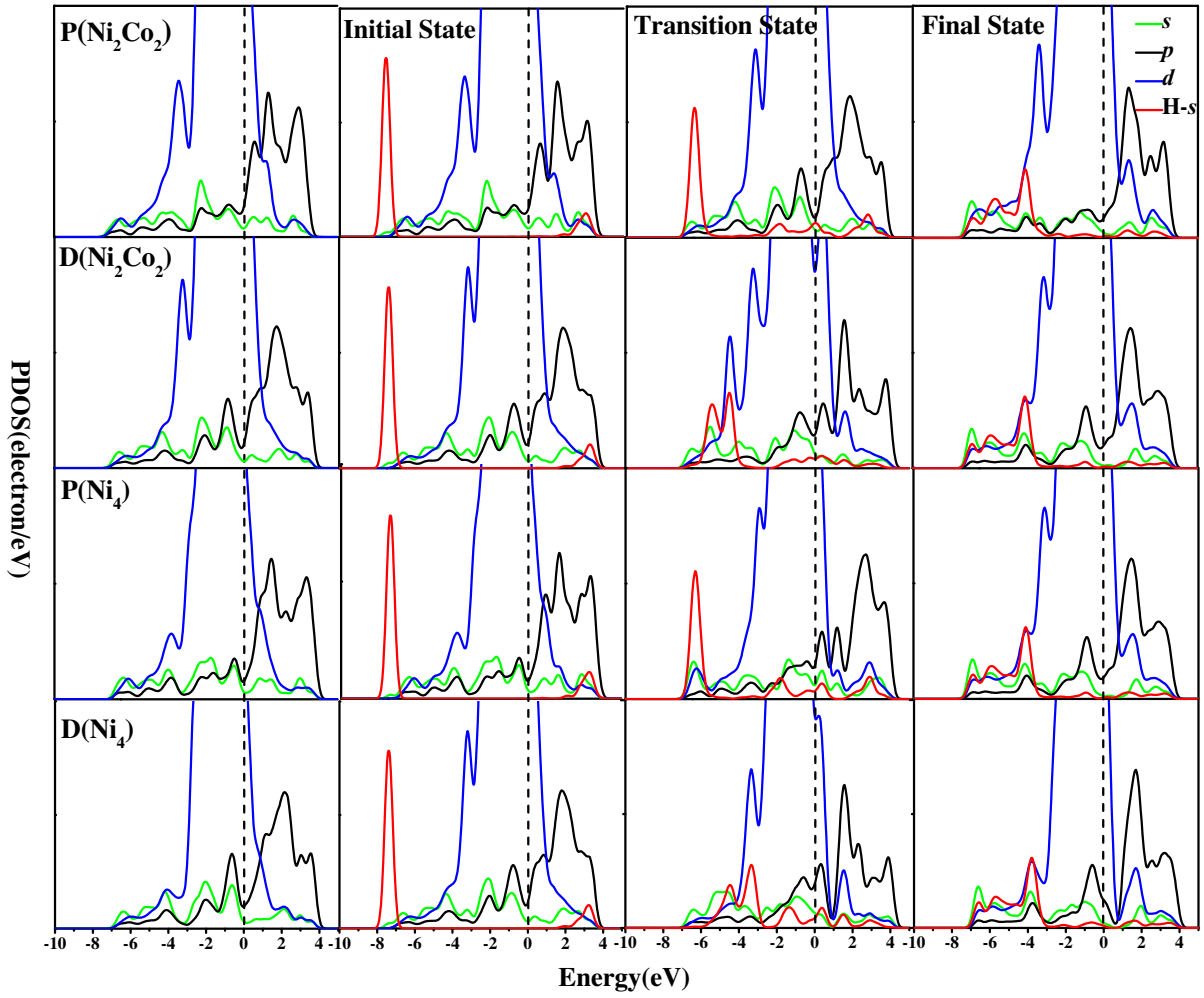

Fig. 8. The PDOS for *s*, *p*, *d*-states of bare Ni_2Co_2 (Ni_4) clusters and the stable Ni_2Co_2 (Ni_4)-Initial States, Transition States, Finial States in the H_2 adsorption–dissociation on the Ni_2Co_2/MgO and Ni_4/MgO. (The location of the dotted line represent the location of the Fermi level).

higher than that on the perfect surface, which are different from the adsorption energies of the single H atom adsorbs on Ni_2Co_2/MgO and Ni_4/MgO. In addition, the deformation energy of the substrate and the metal-support interaction are analyzed and also listed in Table 5. Certainly, the coadsorption energy of two H atoms are also mainly from the interaction between two H atoms and substrate. Analyzing the relationship among E_{MSI} and E_{ads}, we can find that the results are contradictory to those from H adsorption. The increase of interaction in Ni_2Co_2/MgO leads to the increase of coadsorption energy of two H atoms for P(Ni_2Co_2) and D(Ni_2Co_2). In return, the metal-support interaction becomes stronger than that when single H adsorption. For P(Ni_4) and D(Ni_4), the same conclusion can be concluded. On the other hand, when addition Co to Ni/MgO catalysts, the interaction between metal and MgO is decreased, similarly, the adsorption energy of 2H is decreased, the other way round, the interaction between metal and MgO is increased after 2H adsorption.

3.3.3. *Process of H_2 dissociation*

Based on the previous H_2 and 2H adsorption results, the following study is focused on H_2 dissociation on P(Ni_2Co_2) and D(Ni_2Co_2). For further comparison, the H_2 dissociation on the Ni_4/MgO is also studied herein. When H_2 adsorbed on the top of Ni_d atom of P(Ni_2Co_2) and D(Ni_2Co_2) dissociates into two H atoms, the H—H distances are stretched and the H_a—Ni_d and H_b—Ni_d bond are formed, as seen in the transition state structure P(Ni_2Co_2)-TS and D(Ni_2Co_2)-TS in Fig. 7; H_a then moves to the bridge site of Ni_a—Ni_d. Meanwhile, the remaining H_b also moves to the bridge site of Co_c—Ni_d. Certainly, the distance of H—H is longer and the distances of H_a—Ni_d and H_b—Ni_d are shorter on the D(Ni_2Co_2) than on P(Ni_2Co_2) for the transition state structure in H_2 dissociation. Similar dissociation processes happen on P(Ni_4) and D(Ni_4). In addition, the H—H distance is longer for the transition state in H_2 dissociation on D(Ni_4) than that on P(Ni_4).

Table 6
Activation energies (E_a, eV) and reaction energies (ΔE, eV) for H_2 dissociation reactions on the Ni_2Co_2/MgO(001) and Ni_4/MgO(001).

	E_a/eV	ΔE/eV
P(Ni_2Co_2)	0.25	−1.69
D(Ni_2Co_2)	0.14	−1.71
P(Ni_4)	0.45	−1.68
D(Ni_4)	0.37	−1.77

As shown in Table 6, the activation energy barrier of H_2 dissociation on P(Ni_2Co_2) surface is 0.25 eV with an enthalpy change of −1.69 eV. The corresponding energy barrier and enthalpy change on D(Ni_2Co_2) are 0.14 eV and −1.71 eV. For the H_2 dissociation on Ni_4/MgO, the activation barriers are 0.45 and 0.37 eV on P(Ni_4) and D(Ni_4) with enthalpy change of −1.68 and −1.77 eV, respectively. Apparently, the activation energy on D(Ni_2Co_2) is lower than that

on P(Ni_2Co_2). The same result can be obtained for the H_2 dissociation on the Ni_4/MgO. The above results indicate that H_2 dissociation on defective surface is favored as compared to that on perfect surface for the same active component. Simultaneously, based on the results of comparison about the dissociation of H_2 between on Ni_2Co_2/MgO and Ni_4/MgO, one can conclude that the H_2 dissociation is favored on Ni_2Co_2/MgO as compared to that on Ni_4/MgO for the corresponding surface, which indicates that addition of Co to Ni/MgO can improve the catalytic activity.

3.3.4. Effects of MSI on H_2 dissociation

From the above results, one can see that two different MgO supports (perfect and O-vacancy MgO) as well as the addition of a second metal influence the H_2 dissociation on Ni_4/MgO surface. On defective MgO supported Ni_2Co_2, the metal-support interaction is stronger than that on perfect Ni_2Co_2/MgO, which leads to the lower reaction barrier of H_2 dissociation. The same conclusion can be drawn from the Ni_4/MgO catalysts. This suggests that the increase of metal-support interaction can accelerate H_2 dissociation. On the other hand, when addition a second metal Co to Ni catalysts, the metal-support interaction is decreased, correspondingly, accelerating H_2 dissociation. This provides ways to tune the interaction of metal-support in order to modify the catalysts activity, that is, reducing MgO support to produce more oxygen vacancies, or addition a second metal to Ni/MgO, to tune the metal-support interaction, further to improve the catalyst's activity.

3.3.5. PDOS analysis about the process of the H_2 dissociation

To better explore the interaction effect between metal and support on H_2 dissociation process, the project density of state (PDOS) analysis are conducted, as shown in Fig. 8, in which displays the calculated partial density of states projected about the bare Ni_2Co_2 (Ni_4) cluster and those initial state, transition state and final state in the H_2 adsorption-dissociation on Ni_2Co_2/MgO and Ni_4/MgO. The PDOS of the Ni_2Co_2 (Ni_4)-initial state showed that the PDOS peak of *s*-band of H_2 molecule is located around −8.0 eV and the PDOS peak of *d*-band of the metal cluster is above −1 eV. Meanwhile, this is slight overlap area of the *s*-orbital of H_2 and the *s*-, *p*- and *d*-orbital of the metal cluster in the initial state, which indicates that the little interaction between H_2 and metal cluster, further to illustrate the physical absorption of H_2 adsorbed on Ni_2Co_2/MgO and Ni_4/MgO. During the adsorption-dissociation processes, the *s*-orbitals of H_2 shift toward the Fermi level. In the transition state, the overlap areas of the *s*-orbital of H_2 and the *s*-, *p*- and *d*-orbital of the metal cluster are bigger than those in the initial state on all catalysts. However, the overlap areas on D(Ni_2Co_2) and D(Ni_4) are bigger than those on P(Ni_2Co_2) and P(Ni_4), which illustrates the higher activity for H_2 dissociation on metal clusters supported on the defective MgO than that on the perfect MgO. In the final states, it is observable that the strong overlap between two H atoms and the metal, giving rise to the chemical coadsorption state for the two H atoms on the catalysts.

In addition, the order of *d*-band center of Ni or NiCo is not consistent with the reactivity of the H_2 dissociation on P(Ni_4), D(Ni_4), P(Ni_2Co_2) and D(Ni_2Co_2). This may be caused by the interaction of metal-support. This inconsistent was confirmed by Li et al. [31]. Their result demonstrated that the reactivity of the surface metal atom depends not only on its initial state of the *d*-band center, but also on the redistribution of the electrons between the metal cluster and the support upon the adsorption of the adsorption species. Therefore, if the metal atoms are interacting with a particular substrate atom, then the *d*-band center model may fail to predict the reactivity of the catalyst.

4. Conclusions

In this work, we have conducted a DFT-based computational study on the interactions of Ni_2Co_2 with perfect and defective MgO(001) as well as the effects of the interactions on H adsorption and H_2 dissociation compared to those on Ni_4/MgO. DFT calculations show that the interaction between Ni_2Co_2 and oxygen-vacancy MgO are larger than that between Ni_2Co_2 and perfect MgO, which indicates the existence of oxygen vacancy increases the interactions between Ni_2Co_2 and MgO significantly. However, it shows the weaker H chemisorptions and lower H_2 dissociative barrier on defective Ni_2Co_2/MgO than those on the perfect substrates. On the other hand, when addition a second metal Co, the interaction between Ni and MgO is decreased. However, H adsorption is increased, and the dissociation of H_2 accelerates. The present theoretical work indicates it is possible to tune metal-support interaction through addition of a second metal Co or selection a suitable support (such as O-vacancy MgO) to modify the Ni-based catalyst activity.

Acknowledgments

The work was supported financially by the National Natural Science Foundation of China (Nos. 21276171, 21576178) and Doctoral Scientific Research Foundation of Datong University of Shanxi (No. 2012-B-07).

References

[1] S.J. Tauster, S.C. Fung, R.L. Garten, Strong metal-support interactions. Group 8 noble metals supported on titanium dioxide, J. Am. Chem. Soc. 100 (1978) 170–175.
[2] S.J. Tauster, S.C. Fung, R.T.K. Baker, J.A. Horsley, Strong interactions in supported-metal catalysts, Science 211 (1981) 1121–1125.
[3] T. Ohsawa, Y. Matsumoto, H. Koinuma, Combinatorial investigation of transition metals deposited on anatase TiO_2 surface, Appl. Surf. Sci. 223 (2004) 84–86.
[4] W.S.A. Halim, M.M. Assem, A.S. Shalabi, K.A. Soliman, CO adsorption on Ni, Pd, Cu and Ag deposited on MgO, CaO, SrO and BaO: density functional calculations, Appl. Surf. Sci. 255 (2009) 7547–7555.
[5] T.Q. Nguyen, M.C.S. Escaño, H. Nakanishi, H. Kasai, H. Maekawa, K. Osumi, K. Sato, DFT + U study on the oxygen adsorption and dissociation on CeO_2-supported platinum cluster, Appl. Surf. Sci. 288 (2014) 244–250.
[6] Y.H. Hu, E. Ruckenstein, Binary MgO-based solid solution catalysts for methane conversion to syngas, Catal. Rev. 44 (2002) 423–453.
[7] Y.H. Hu, E. Ruckenstein, The characterization of a highly effective NiO/MgO solid solution catalyst in the CO_2 reforming of CH_4, Catal. Lett. 43 (1997) 71–77.
[8] Y.H. Hu, E. Ruckenstein, An optimum NiO content in the CO_2 reforming of CH_4 with NiO/MgO solid solution catalysts, Catal. Lett. 36 (1996) 145–149.
[9] E. Ruckenstein, Y.H. Hu, The effect of precursor and preparation conditions of MgO on the CO_2 reforming of CH_4 over NiO/MgO catalysts, Appl. Catal. A 154 (1997) 185–205.
[10] H.A.E. Dole, A.C. Costa, M. Couillard, E.A. Baranova, Quantifying metal support interaction in ceria-supported Pt, PtSn and Ru nanoparticles using electrochemical technique, J. Catal. 333 (2016) 40–50.
[11] K. Larmier, C. Chizallet, P. Raybaud, Tuning the metal-support interaction by structural recognition of cobalt-based catalyst precursors, Angew. Chem. Int. Ed. 54 (2015) 6824–6827.
[12] F. Liao, T.W.B. Lo, J. Qu, A. Kroner, A. Dent, S.C.E. Tsang, Tunability of catalytic properties of Pd-based catalysts by rational control of strong metal and support interaction (SMSI) for selective hydrogenolyic CC and CO bond cleavage of ethylene glycol units in biomass molecules, Catal. Sci. Technol. 5 (2015) 3491–3495.
[13] Y. Wang, E. Florez, F. Mondragon, T.N. Truong, Effects of metal-support interactions on the electronic structures of metal atoms adsorbed on the perfect and defective MgO(100) surfaces, Surf. Sci. 600 (2006) 1703–1713.
[14] A. Djaidja, H. Messaoudi, D. Kaddeche, A. Barama, Study of Ni-M/MgO and Ni-M-Mg/Al (M=Fe or Cu) catalysts in the CH_4-CO_2 and CH_4-H_2O reforming, Int. J. Hydrogen Energy 40 (2015) 4989–4995.
[15] J. Zhang, H. Wang, A.K. Dalai, Development of stable bimetallic catalysts for carbon dioxide reforming of methane, J. Catal. 249 (2007) 300–310.
[16] M.M. Hossain, K.E. Sedor, H.I. de Lasa, Co-Ni/Al_2O_3 oxygen carrier for fluidized bed chemical-looping combustion: desorption kinetics and metal-support interaction, Chem. Eng. Sci. 62 (2007) 5464–5472.

[17] D. Cui, J. Liu, J. Yu, J. Yue, F. Su, G. Xu, Necessity of moderate metal-support interaction in Ni/Al_2O_3 for syngas methanation at high temperatures, RSC Adv. 5 (2015) 10187–10196.
[18] T. Mineva, V. Alexiev, C. Lacaze-Dufaure, E. Sicilia, C. Mijoule, N. Russo, Periodic density functional study of Rh and Pd interaction with the (100) MgO surface, J. Mol. Struct. 903 (2009) 59–66.
[19] D.C. Koningsberger, B.C. Gates, Nature of the metal-support interface in supported metal catalysts: results from X-ray absorption spectroscopy, Catal. Lett. 14 (1992) 271–277.
[20] S. Martin, R. Thomas, M. Pozzoni Umberto, G. Livia, H. Markus, R. Hans-Peter, P. Gianfranco, F. Hans-Joachim, Control of the charge state of metal atoms on thin MgO films, Phys. Rev. Lett. 98 (2007) 096107.
[21] S.S. Rath, N. Sinha, H. Sahoo, B. Das, B.K. Mishra, Molecular modeling studies of oleate adsorption on iron oxides, Appl. Surf. Sci. 295 (2014) 115–122.
[22] R. Zhang, B. Wang, H. Liu, L. Ling, Effect of surface hydroxyls on CO_2 hydrogenation over Cu/γ-Al_2O_3 catalyst: a theoretical study, J. Phys. Chem. C 115 (2011) 19811–19818.
[23] W. Li, X.M. Lu, G.Q. Li, J.J. Ma, P.Y. Zeng, J.F. Chen, Z.L. Pan, Q.Y. He, First-principle study of SO_2 molecule adsorption on Ni-doped vacancy-defected single-walled (8, 0) carbon nanotubes, Appl. Surf. Sci. 364 (2016) 560–566.
[24] P.V. Sushko, A.L. Shluger, C.R.A. Catlow, Relative energies of surface and defect states: ab initio calculations for the MgO(001) surface, Surf. Sci. 450 (2000) 153–170.
[25] F. Leroy, C. Revenant, G. Renaud, R. Lazzari, In situ GISAXS study of the growth of Pd on MgO(001), Appl. Surf. Sci. 238 (2007) 233–237.
[26] A.V. Matveev, K.M. Neyman, I.V. Yudanov, N. Rösch, Adsorption of transition metal atoms on oxygen vacancies and regular sites of the MgO (001) surface, Surf. Sci. 426 (1999) 123–139.
[27] Z. Liu, Y. Wang, J. Li, R. Zhang, The effect of γ-Al_2O_3 surface hydroxylation on the stability and nucleation of Ni in Ni/γ-Al_2O_3 catalyst: a theoretical study, RSC Adv. 4 (2014) 13280–13292.
[28] C. Wang, Y. Chen, T. Li, B. Yao, Composition design and laser cladding of Ni-Zr-Al alloy coating on the magnesium surface, Appl. Surf. Sci. 256 (2009) 1609–1613.
[29] M. Zhang, J. Chen, Y. Yu, Y. Zhang, DFT study on the structure of Ni/α-Al_2O_3 catalysts, Appl. Surf. Sci. 287 (2013) 97–107.
[30] H. Liu, B. Teng, M. Fan, B. Wang, Y. Zhang, H. Gordon Harris, CH_4 dissociation on the perfect and defective MgO(001) supported Ni_4, Fuel 123 (2014) 285–292.
[31] J. Li, E. Croiset, L. Ricardez-Sandoval, Effect of metal-support interface during CH_4 and H_2 dissociation on Ni/γ-Al_2O_3: a density functional theory study, J. Phys. Chem. C 117 (2013) 16907–16920.
[32] K. Takanabe, K. Nagaoka, K. Nariai, K. Aika, Titania-supported cobalt and nickel bimetallic catalysts for carbon dioxide reforming of methane, J. Catal. 232 (2005) 268–275.
[33] M.D. Segall, P.J.D. Lindan, M.J. Probert, C.J. Pickard, P.J. Hasnip, S.J. Clark, M.C. Payne, First-principles simulation: ideas illustrations and the CASTEP code, J. Phys.—Condens. Mater. 14 (2002) 2717–2744.
[34] V. Milman, B. Winkler, J.A. White, C.J. Pickard, M.C. Payne, E.V. Akhmatskaya, R.H. Nobes, Electronic structure, properties, and phase stability of inorganic crystals: a pseudopotential plane-wave study, Int. J. Quantum. Chem. 77 (2000) 895–910.
[35] H. Liu, R. Zhang, R. Yan, B. Wang, K. Xie, CH_4 dissociation on NiCo(111) surface: a first-principles study, Appl. Surf. Sci. 257 (2011) 8955–8964.
[36] J.P. Perdew, K. Burke, M. Ernzerhof, J.P. Perdew, K. Burke, M. Ernzerhof, Generalized gradient approximation made simple, Phys. Rev. lett. 77 (1996) 3865.
[37] H.J. Monkhorst, J.D. Pack, Special points for brillouin-zone integrations, Phys. Rev. B 13 (1976) 5188–5192.
[38] B. Hammer, J.K. Nørskov, Electronic factors determining the reactivity of metal surfaces, Surf. Sci. 343 (1995) 211–220.
[39] M. Mavrikakis, B. Hammer, J.K. Nørskov, Effect of strain on the reactivity of metal surfaces, Phys. Rev. Lett. 81 (1998) 2819–2822.
[40] F.B.M. Van Zon, S.D. Maloney, B.C. Gates, D.C. Koningsberger, Structure and nature of the metal-support interface: characterization of iridium clusters on magnesium oxide by extended x-ray absorption fine structure spectroscopy, J. Am. Chem. Soc. 115 (1993) 10317–10326.
[41] B. Wang, R. Yan, H. Liu, Effects of interactions between NiM (M=Mn, Fe Co and Cu) bimetals with MgO(100) on the adsorption of CO_2, Appl. Surf. Sci. 258 (2012) 8831–8836.
[42] Y.F. Zhukovskii, E.A. Kotomin, G. Borstel, Adsorption of single Ag and Cu atoms on regular and defective MgO(001) substrates: an ab initio study, Vacuum 74 (2004) 235–240.
[43] N. Lopez, J.C. Paniagua, F. Illas, Controlling the spin of metal atoms adsorbed on oxide surfaces: ni on regular and defective sites of the MgO(001) surface, J. Chem. Phys. 117 (2002) 9445–9451.
[44] Y. Wang, Y. Su, M. Zhu, L. Kang, Mechanism of CO methanation on the Ni_4/γ-Al_2O_3 and Ni_3Fe/(-Al_2O_3 catalysts: a density functional theory study, Int. J. Hydrogen Energy 40 (2015) 8864–8876.
[45] L.N. Kantorovich, J.M. Holender, M.J. Gillan, The energetics and electronic structure of defective and irregular surfaces on MgO, Surf. Sci. 343 (1995) 221–239.
[46] T. Urano, T. Kanaji, M. Kaburagi, Surface structure of MgO(001) surface studied by LEED, Surf. Sci. 134 (1983) 109–121.
[47] W.R. Welton-Cook, W. Berndt, A LEED study of the MgO(100) surface: identification of a finite rumple, J. Phys. C: Solid State Phys. 15 (1982) 5691–5710.
[48] A.J. Martin, H. Bilz, Charge deformation and geometric relaxation at the (001) MgO surface, Phys. Rev. B 19 (1979) 6593–6600.
[49] G.L. Haller, D.E. Resasco, Metal-support interaction: group VIII metals and reducible oxides, Adv. Catal. 36 (1989) 173–235.
[50] J.M. Herrmann, M. Gravelle-Rumeau-Maillot, P.C. Gravelle, A microcalorimetric study of metal-support interaction in the $PtTiO_2$ system, J. Catal. 104 (1987) 136–146.